International Journal of Science and Engineering Applications
Volume 12-Issue 04, 79 - 85, 2023, ISSN:- 2319 - 7560
DOI: 10.7753/IJSEA1204.1028

Development of a Bipolar Marx Pulse Generator Using Buck-Boost Converter

Saber Roshan
Power & Control Department
Shiraz University
Shiraz, Iran

Mehdi Allahbakhshi
Power & Control Department
Shiraz University
Shiraz, Iran

Ebrahim Farjah
Power & Control Department
Shiraz University
Shiraz, Iran

Teymoor Ghanbari
School of Advanced Technologies
Shiraz University
Shiraz, Iran

Abstract: A new structure of the Marx pulse generator for generating bipolar high-voltage pulses is introduced. This structure is composed of a buck-boost converter and connected to a low DC voltage source and several parallel diode-capacitor units. In the first stage, the inductor energy is supplied through the voltage source and in the next stage, the inductor energy is transferred to capacitors. For generating the pulses, voltage polarities of the capacitors are changed by a small inductor which is in resonant with the capacitors. Then, using a fast switch, the capacitors are connected in series to generate desirable high-level pulses. To have bipolar pulses, polarity of capacitors is inverted, alternatively. Modularity of the proposed structure enables us to increase number of the units for generating higher voltage level, straightforwardly.

Keywords: pulse generator; electric polarization; Marx pulse generator; bipolar high-voltage pulses; negative buck-boost converter; resonant circuit.

NOMENCLATURE

T	Period of switching
T_{C^+}	Charging time of capacitors
T_{C^-}	Required time for resonance
V_{in}	Magnitude of input voltage
L_1	Inductance of the main inductor
$L_1 - L_{\text{n}}$	Inductance of the resonant inductor
C_{S}	Equivalent capacitance of the capacitors in series connection
C	Equivalent capacitance of the capacitors in parallel connection
R	load resistor
I_{L}	Maximum current of inductor L_1
ΔT	Duration of charging L_1
V_{on}	On-state voltage of the semiconductor components (switches or diodes)
I_{SW}	Current of the semiconductors
R_{on}	On-state resistance of the Semiconductors
$I_{\text{SW,avg}}$	Average current of the semiconductor
$I_{\text{SW,rms}}$	Effective current of the semiconductor
$V_{\text{SW,on}}$	Semiconductors' voltage before turning on
$I_{\text{SW,on}}$	Semiconductors' current after turning on
$V_{\text{SW,off}}$	Semiconductors' voltage after turning off
$I_{\text{SW,off}}$	Semiconductors' current before turning off
L_C	DC line inductance
$T_{\text{on,SW}}$	Semiconductors' turning-on duration
$T_{\text{off,SW}}$	Semiconductors' turning-off duration

1. INTRODUCTION

High-voltage pulse generators are used in different applications such as plasma, lasers feeding, minerals corrosion, food industries, water and wastewater treatment, military and medical industries [1]–[4]. The generated pulses by the mentioned equipment are either unipolar or bipolar types. Bipolar high-voltage pulses are more efficient in industrial processes like processing and sterilizing foodstuffs, purification of water, and air pollution. Using a pulsating electric field with high enough power, one can penetrate cell membrane to kill microbes, called electric polarization [5]. In recent decades, this method has been introduced as an alternative approach for sterilizing foodstuffs and liquid materials instead of the old conventional methods. This approach needs bipolar pulse generators [6], [7] as the main core of the method.

The pulse generators can be classified into two main groups including classic and modern pulse generators. In the classic pulse generators, like multilevel Marx pulse generator, spark gap switches are utilized for the switching. Such switches make them big, inefficient, and expensive.

Modern pulse generators are based on semiconductor switches. The main advantages of these switches can be mentioned as low volume, high efficiency, high reliability, long lifespan, low cost, and high switching frequency which, enables them to generate pulses with high repetition.

Basic structure of the Marx generators has some challenges such as low reliability, bulky dimensions, high cost, low repetition rate, and short lifespan and the capacitors used in this structure can be charged maximum to the DC voltage source level[8], [9]. In new types of Marx generators, in which solid state switches are used instead of the resistors and spark gap switches, the capacitors can be charged up simultaneously to Vin, twice of Vin, or even several times of Vin. Solid-state switches-based pulse generators are suitable options for tackling the mentioned challenges. Although Marx generators with solid-state switches have acceptable performance, new structures can be presented to promote the performance of these pulse generators.

International Journal of Science and Engineering Applications
Volume 12-Issue 04, 79 - 85, 2023, ISSN:- 2319 - 7560
DOI: 10.7753/IJSEA1204.1028

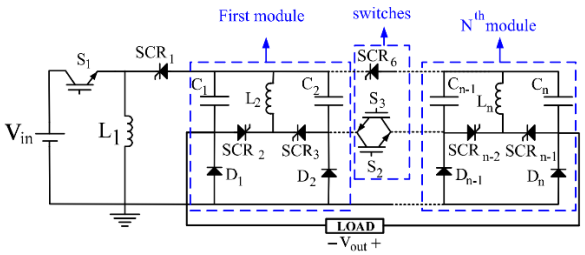

Fig.1. N-stage circuit of the proposed bipolar MG.

Marx topology as a suitable structure for generating several kilovolts pulses, can also be divided into unipolar and bipolar. In [9-20], some unipolar pulse generators have been presented. In the structures presented in [10]–[13], the capacitors are charged up to DC voltage source. Therefore, a high-level DC source or many capacitor stages are needed for generating higher output voltages.

In order to reduce switching losses in power electronics, zero voltage switching (ZVS) and zero current switching (ZCS) are provided. In pulse generators, this target has been followed up, as well. In [14], [15], using an inductor in series with the capacitors and DC source, the capacitors can be charged up to twice of source voltage, as a result, the number of units required capacitive or DC supply voltage level is reduced. Another merit of this structure is realizing ZCS.

In recent years, many researches have been dedicated to the pulse generators in which dc-dc converters are utilized to improve their performance [16]. In the structures presented in [17]–[20], the capacitor units are charged up to several times of the source voltage using a buck-boost converter. It should be mentioned that the voltage of the circuit components arises in this condition, so the number of capacitor stages is determined considering this over voltage. In [16] and [17], a positive buck-boost converter has been used for this purpose. In [16], an inductor unit has been utilized for charging all of the capacitor units. Output of this pulse generator is a unipolar high-voltage needle pulse which has a great deal of flexibility and generation in high frequency. In [17], less elements have been employed in the proposed structure in respect with the other Marx generators. However, it has more operation modes, which results in reduction of the repetition frequency. In [18], renewable energy sources are connected through an interlinking converter with considering reduction in leakage current issue. These low cost, high efficiency converters have very useful applications in microgrids[18].

In [19],[20], two modular structures have been suggested in which negative buck-boost converter was exploited. In [19], for charging the inductor, one source with H type switching has been used. In each cycle of the pulse generation, inductor is charged two times, one for the odd capacitors and the other for the even capacitors. In [20], the capacitors are charged simultaneously through the inductor unit and it includes three operation modes that make it capable of generating pulses with higher frequency in comparison with the other structures. In the pulse generators in which buck-boost converter is utilized, switching losses of the generators can be reduced by operation of the converters in discontinues conduction mode.

In [21], [22], some bipolar Marx generators have been presented. The proposed structure in [21] is a development of structure of [10], in this structure, there are six switches per capacitor unit. In [22] a two level converter is considered for grounding aspects. In [23], the number of switches has reduced to five and four switches for each capacitor unit, respectively.

In [24], two DC sources have been employed in order to reduce the number of the switches. One of the DC sources charges the odd capacitors and the other one charges even capacitors, which results considerable reduction in the number of switches. However, during discharging of the capacitor units, always one of them could not be discharged. During pulse generation, voltage on the DC source can be reached (n-1)Vc. Therefore, an inductor-resistor unit is located in the path of source and the capacitor units to prevent the over voltage on the source. In higher voltages, value of inductor-resistor unit should be increased, which results in slowing down the charging processes and decreasing repetition frequency of the circuit. Capacitor units in the structures of [21], [23]–[25], can be charged up to DC source value. Therefore, they have the same problems like unipolar generators. In [26], a unipolar/bipolar structure has been introduced, in which a buck-boost converter is utilized for charging the capacitors up to several times of the DC source voltage. Also, different power quality issues like voltage sag can be reduced by the method proposed in [25]. This structure exploits two inductors as energy storage, one for positive pulses generation and another one for negative pulses generation [27]. Although in this structure, the number of elements was reduced considerably, it is able to generate only a bipolar pulse for one capacitor unit and does not have modular capability.

Considering the mentioned limitations in bipolar pulse generators, a novel structure of these generators is presented in this paper. In the proposed structure, a negative buck-boost converter is used for charging the capacitor units. The structure is modular based and each module includes two capacitors, one inductor, two thyristors and two diodes. The polarity of capacitors changes in a resonant condition. Both capacitors are connected to the inductor through the switches [28]. After charging the capacitors, polarity of the odd capacitors is changed through a resonant circuit for generating positive pulses. In case of generating negative pulse, polarity of even capacitors is changed. Circuit operation, design requirements and efficiency of the proposed topology are addressed in details. Performance of the proposed pulse generator is investigated by some simulations at Matlab/Simulink. Also, a comparison between the performance of the reported bipolar structures in the literature and the proposed structure is presented.

2. THE PROPOSED BIPOLAR PULSE GENERATOR

The proposed n-level bipolar pulse generator structure is shown in Fig. 1. Procedure of the bipolar pulse generation is divided into two stages: common and non-common operation stages. The common stage is carried out twice per operation cycle, while the non-common is performed once per cycle. In the following, the procedure of the bipolar pulse generation is discussed in details:

2.1 Common Operation Stage

Pulse generation is realized in two stages as follows:
First stage (Charging the inductor during ΔT): In the first stage, shown in Fig. 2 (a), the main inductor, located at the input of the converter, is connected to the DC source through S_1 and charged for duration ΔT. The charged inductor plays the role of a current source. According to Equation (1), maximum inductor current in ΔT will reach I_L. In this time interval, the diodes and thyristor 1 prevent current to pass through the capacitor units. All semiconductor devices, such as IGBTs, SCRs, and diodes are assumed to be ideal. So, voltage drop on each of these components is zero during conduction.

International Journal of Science and Engineering Applications
Volume 12-Issue 04, 79 - 85, 2023, ISSN:- 2319 - 7560
DOI: 10.7753/IJSEA1204.1028

$$V_{dc} = L.\frac{IL}{\Delta T} \rightarrow IL = \frac{V_{dc}.\Delta T}{L} \quad (1)$$

Second Stage (The energy is transferred from the inductor to the capacitors): According to Fig. 2 (b), in the beginning of this stage, thyristors 1 and 6 and the diodes are turned on. According to Equations (2), during Tc^+, the stored energy in the inductor is transferred to capacitors C_i, and all four capacitors are charged to $V_{C,max}$. Upon the inductor current reaches zero (at the end of Tc^+), all the diodes and thyristors 1 and 6 are turned off simultaneously and the capacitors remain at voltage $V_{C,max}$. By assuming C1= C2= C3 =C4 = C, we have:

$$i_L(t) = I_L \times cos(\frac{t}{\sqrt{L \times 4C}}) \xrightarrow{\overrightarrow{i_L(t)=0}} T_c{+}= t = \frac{\pi}{2}\sqrt{L \times 4C}$$

$$V_C(t) = I_L\sqrt{\frac{L}{4C}} \times sin(\frac{t}{\sqrt{L\times 4C}}) \xrightarrow{V_C(Tc+)} V_{C,Max} = I_L\sqrt{\frac{L}{4C}} \quad (2)$$

While thyristor 1 is off, the inductor unit is separated from the capacitor unit. Thus, the inductor can be recharged again.

2.2 Uncommon Operation Stage

First Stage (Altering polarity of the odd capacitors): When the inductor current reaches zero and whole the energy is transferred from the inductor to the capacitors, as shown in Fig. 2(c), polarities of the capacitors 1 and 3 are changed to generate positive pulse. To do so, thyristors 2 and 4 are turned on simultaneously to create a loop between the inductors and capacitors. In this condition, energy of the capacitors transfers to the inductors. Then, the inductors discharge their stored energy to the initial charging current direction. In this condition, the capacitors will be charged from top to bottom direction of the circuit, again. Now, voltage of each capacitor is $V_{C,max}$, but with the opposite polarities. After charging the capacitors, current of the inductors reaches zero and thyristors 2 and 4 will be turned off. In this state, current Equations of inductors L_2 and L_3 as well as capacitors C_1 and C_3 are:

$$i_{L_r^{(2,3)}}(t) = V_{C,max\times}\sqrt{\frac{C}{L_r}}sin(\frac{t}{\sqrt{L\times 4C}}) \xrightarrow{i_{L_r}^{(t)}=0} t = T_{C^-} = \pi\sqrt{L_r \times C} \quad (3)$$

$$v_{C_{1,3}}(t) = V_{C,max}\, cos(\frac{t}{\sqrt{L_r\times C}}) \xrightarrow{t=T_{C^-}} v_{C_{1,3}}(t) = -v_{C,\max} \quad (4)$$

According to Equation (3), current of inductors L_2 and L_3 reaches zero after Tc^-. Δt this time, the capacitors voltages reach maximum negative value.

Second Stage (Generation of positive pulse): In this stage, according to Fig. 2 (d), polarities of the odd capacitors are changed and the voltage across each of the four capacitors is $V_{C,max}$. Also, the polarity of all capacitors is desirable for connecting in series. Upon, S_2 is turned on, the capacitors are connected in series and the summation of all the capacitors voltages is applied to the output. In this stage all the diodes are turned off under reverse bias of the capacitors' voltages. Thus, the output voltage is equal to:

$$V_{out}(t) = v_{C_1} + v_{C_2} + v_3 + v_4 = 4 \times v_{C,max} = 4IL\sqrt{\frac{L}{4C}} \quad (5)$$

The capacitors are discharged by time constant T=5RC_S. Third Stage (Changing polarity of the even capacitors): at the beginning of this stage, the common operation stage should be performed once again. The capacitors are charged and when the inductor current reaches zero, according to Fig. 2 (e), thyristors 1 and 5 are turned on at the same time to change the polarity of capacitors C_2 and C_4 and generate negative pulse. The same as the procedure mentioned in the first stage, current Equations of inductors L_2 and L_3, and capacitors C_2 and C_4 are the same as Equations (3) and (4). Also, thyristors 1 and 5 are automatically turned off when inductors current reaches zero.

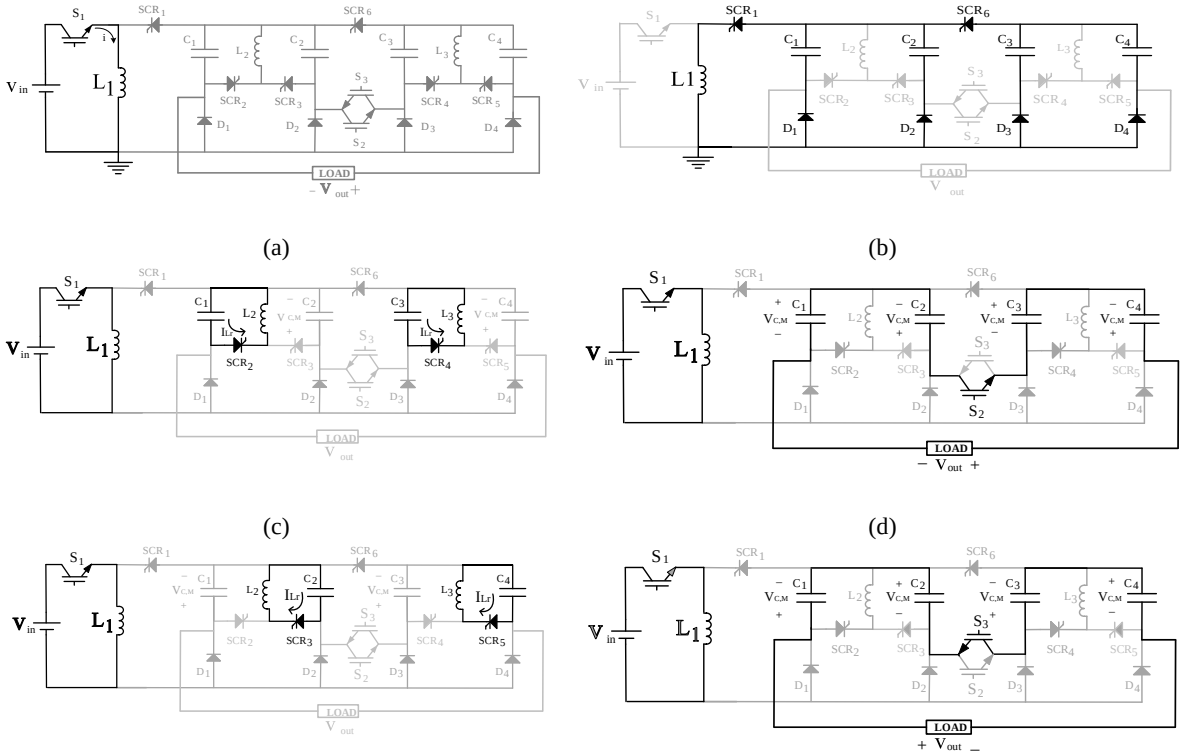

Fig. 2. Switching modes for bipolar pulse generator .a) The main inductor charging b) Capacitor units charging and the main inductor discharging c) Polarity changing of odd capacitors d) positive pulse generation e) Polarity changing of even capacitors f) negative pulse generation.

International Journal of Science and Engineering Applications
Volume 12-Issue 04, 79 - 85, 2023, ISSN:- 2319 - 7560
DOI: 10.7753/IJSEA1204.1028

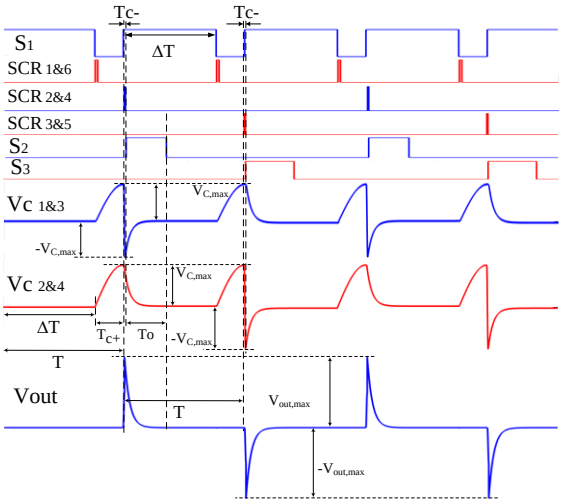

Fig. 3. Switching control strategy, voltages of capacitor and output.

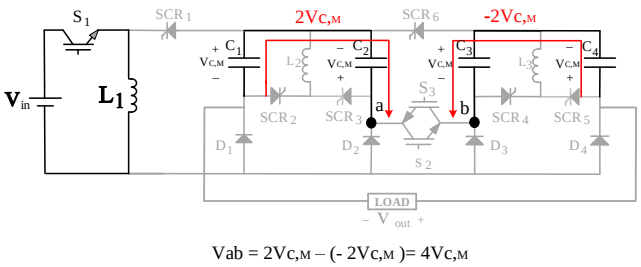

Vab = 2Vc,M – (- 2Vc,M)= 4Vc,M

Fig. 4. Voltage of switches S_2 and S_3 during positive pulse generation.

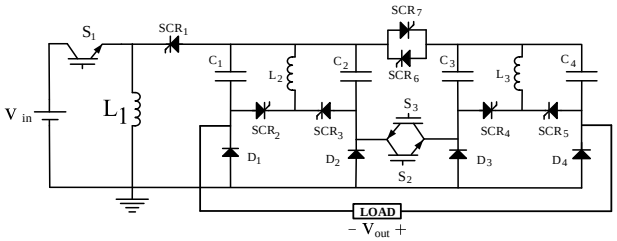

Fig. 5. The proposed structure for decreasing the voltage of S_2 and S_3.

Fourth Stage (Generation of negative pulse): In this stage, according to Fig. 2 (f), polarities of the even capacitors are changed, while voltage across each of the four capacitors is $V_{C,max}$. By turning on switch S_3, the output voltage will be equal to the sum of series capacitors ($4V_{C,max}$). Therefore, the output voltage is the same as Equation (5). Also, all the diodes are turned off due to reverse-biased of the capacitors voltages and the capacitors are discharged by time constant T_O.

2.3 Switches Control Strategy

According to Fig. 3, during ΔT, S_1 is turned on and the inductor current reaches I_L by voltage + V_{in}. After ΔT, S_1 is turned off and SCR_1 is turned on simultaneously. All the capacitors are charged by turning on SCR_1 (energy is ransferred from the inductor to the capacitors). In this topology, the switching is designed in a way that all the capacitors are charged at the same time. After T_{C+}, SCR_1 is automatically turned off when its current reaches zero. When thyristor 1 is turned off, all the diodes are reverse-biased due to the capacitors' voltages. In this condition, the inductor unit is separated from the capacitors' units. So, the inductor charging gets started simultaneous with switching of the capacitor unit. In order to generate positive pulse, SCR_1 and SCR_2 are turned on and by forming a resonant circuit, polarities of the capacitors' voltages change. After changing the capacitors polarities, the inductors and thyristors current reaches zero. Therefore, these thyristors are turned off automatically. Now, polarities of the capacitors are suitable for connecting in series by turning on S_2 to generate voltage with positive polarity. Then, in order to generate negative voltage, polarities of capacitors C_2 and C_4 are changed by turning on SCR_3 and SCR_5 and connecting the capacitors in series by S_3 .

2.4 Switches Control Strategy

As mentioned, after changing the polarity, two capacitors are located at both side of switches S_2 and S_3 , which are connected in series. As a result, in both generating positive and negative pulses, a voltage equal to $4V_{C,max}$ is applied across these switches. Therefore, in order to reduce this voltage, according to Fig. 5, by adding a parallel thyristor to thyristor 6, in the opposite direction and modifying control strategy of thyristor switch 6, this voltage is reduced to $2V_{C,max}$.

In generating positive pulse state, thyristor 2, 4, and 7 are turned on at the same time. According to Fig 6. (a), simultaneous with changing polarity of the odd capacitors, summation of C_1 and C_4 voltages are applied across the load. So, voltage across switches S_2 and S_3 will be reduced. In generating negative pulse as shown in Fig 6. (b), simultaneous with turning thyristors 3 and 5 on, thyristor 6 is also turned on. Therefore, according to the prior state, voltage across switches S_2 and S_3 is reduced, as shown in Fig. 7.

3. COMPARISON OF THE PROPOSED STRUCTURE WITH THE OTHER SIMILAR STRUCTURES

In this part, number of the employed components, capacitors voltages, and output voltage of the proposed structure are compared with three structures that are capable of generating both unipolar and bipolar pulses, as shown in Table 1.

In the proposed structures in [10,13], capacitor units could only be charged to DC source, so in order to generate higher voltage, number of capacitor levels should be increased or a bigger DC source should be used. Both these remedies result in increment in cost and volume of the generator. In these structures, voltage of the capacitor cannot be used for increasing the output

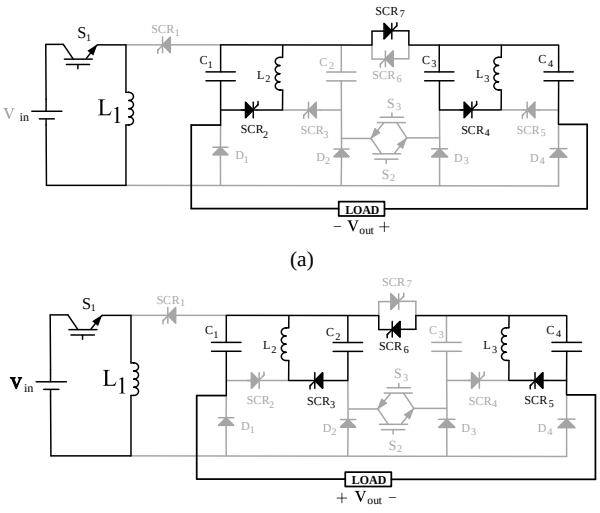

Fig. 6. The polarity changing of odd and even capacitors, and increasing the output voltage to $2V_{Cmax}$.

International Journal of Science and Engineering Applications
Volume 12-Issue 04, 79 - 85, 2023, ISSN:- 2319 - 7560
DOI: 10.7753/IJSEA1204.1028

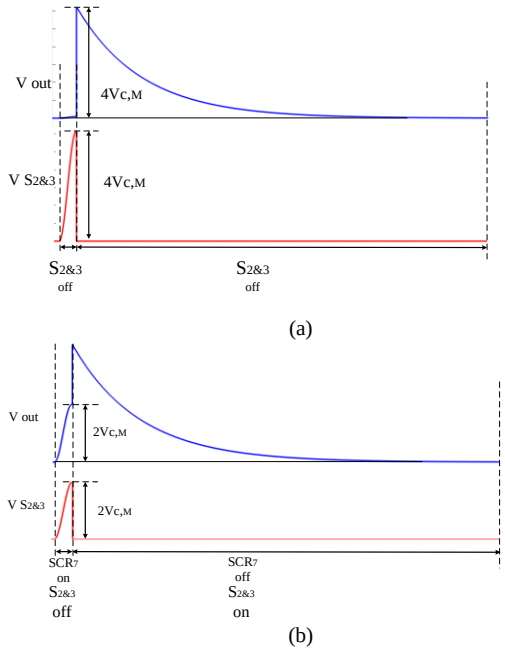

Fig. 7. The effect of the switch added to the circuit on the output voltage and voltage of switches S_2 and S_3.

voltage. From number of the used switches point of view, structure of [10] has more switches than the proposed structure. The structure of [13] has a smaller number of switches than the proposed structure, but in this structure two DC sources have been used to reduce the number of the switches which is a drawback. Also, there is no switch to charge the capacitors unit, so charging control could not be carried out appropriately. In [14], the problem of low stored energy in the capacitor units has been solved by using a buck-boost converter, but adding the converter increases switching frequency of the structure. In this structure like the proposed structure, voltage of all the capacitors can be exploited for generating high output voltage. Power electronics components could tolerate a permissible voltage. Maximum voltage of the components in the proposed structure in off state are tabulated in Table 2. It can be observed that in this structure, maximum voltage is applied across the diodes at the end and beginning of the circuit, which can be alleviated by connecting some diodes in series. Among the switches, maximum voltage is applied across SCR_1.

4. ANALYZING EFFICIENCY AND LOSSES OF THE PROPOSED STRUCTURE

Losses of the proposed structure includes switching and conduction losses. Equations for input power (P_{in}), conduction losses (P_C), and switching losses (P_{sw}) are presented in (6-8).

$$P_{in} = \frac{1}{T}\int_T V_{in} I_L (dt) = \frac{1}{T} V_{in} I_L \Delta T \quad (6)$$

$$P_C = \frac{1}{T}\int_T (V_{on} I_{sw} + R_{on} I_{sw}^2)(dt) = V_{on} I_{sw,avg} + R_{on} I_{sw,rms}^2 \quad (7)$$

$$P_{sw} = \frac{1}{T}\int_T (V_{sw,on} I_{sw,on} + V_{sw,off} I_{sw,off})(dt) \quad (8)$$

SCR_1 and SCR_6 are turned on in the stage of transferring energy from inductor L_1 to the capacitor units and at zero voltage. S_2 and S_3 are also turned on at zero voltage and when the capacitors are fully discharged (after 5τ). At zero current, these two switches are turned off. Thus, switching losses for SCR_1, SCR_6, S_2 and S_3 are negligible. Switching losses for all the diodes are about zero due to zero voltage and zero current switching.

Table 1. Comparing the Number of the Proposed Structure Devices with Three other Refrences.

	PROPOSED GENERATOR		[10]	[13]	[14]
Number of Switches	First state	Second state	17	8	20
	9	10			
Number of Diodes	4		8	5	12
Number of Inductor	3		0	2	2
Number of Capacitor	4		4	4	4
Number of DC Source	1		1	2	1
V_C	$I_L\sqrt{\frac{L}{4C}}$		V_{dc}	V_{dc}	$LI_0 e^{\alpha t}\left(\frac{\alpha^2+\beta^2}{\beta}\sin\beta t\right)$
V_{out}	$4I_L\sqrt{\frac{L}{4C}}$		$4V_{dc}$	$4V_{dc}$	$v_{out} = nv_{cn}$

Efficiency of the proposed structure depends on input voltage magnitude and output resistor, which is calculated in different conditions as shown in Fig. 8.

The efficiency is calculated considering the specifications presented in Table 3 by assuming that voltage drop and resistance of all the switches in conduction mode are 2.5 volts and 5 mΩ. Switching losses of S_1 is calculated assuming that turning on and off duration of this switch are 50 ns and 150 ns, respectively. Power losses for a period of operation is obtained from Equation (9).

$$P_L = 2Pc_{S1} + 2Pc_{SCR1} + 2Pc_{SCR6} + 2Pc_{S2} + 4Pc_{SCR2} + 8P_D + 2Psw_{S1} \quad (9)$$

The efficiency can be improved by increasing output resistor, but increasing the resistor also raises To. Increasing To causes switches S_2 and S_3 not to be disconnected at zero current anymore.

5. SIMULATION RESULTS

In order to compare the simulation results, all parameters are considered according to table 4. The structure is simulated in MATLAB-SIMULINK. The DC source has a constant voltage 10 volts. Duration for charging inductor L_1 is 30 us and the inductor current at the end of this duration is equal to 0.15 A.

Table 2. Maximum Voltage and Current for Switching Devices in the Proposed Structure.

Structure elements	First State	Second State
S_1	$V_{dc} + V_{C.max}$	
S_2, S_3	$4V_{C.max}$	$2V_{C.max}$
S_{CR1}	$3V_{C.max} - V_{in}$	
SCR_{2-5}	$2V_{C.max}$	
$SCR_{6,7}$	$2V_{C.max}$	
D_1 & D_4	$4V_{C.max}$	
D_2 & D_3	$2V_{C.max}$	

International Journal of Science and Engineering Applications
Volume 12-Issue 04, 79 - 85, 2023, ISSN:- 2319 - 7560
DOI: 10.7753/IJSEA1204.1028

Table 3. The Equations of Switching and Conduction Losses in the Proposed Structure.

Structure elements	SWITCHING LOSSES (P_{sw})	Conduction losses (P_C)
S_1	$\frac{I_L V_{on,sw} \Delta T}{2T} + \frac{I_L{}^2 R_{on,sw} \Delta T}{3T}$	$\frac{I_L V_{in} t_{on,sw}{}^2}{2T\,\Delta T} + \frac{I_L V_{in} t_{off,sw}}{2T}$
S_2, S_3	0 (Soft Switching)	$\frac{V_{out} V_{on,sw} C_{eq,ser}}{T}\left(1-e^{-5}\right) + \frac{V_{out}{}^2 R_{on,sw} C_{eq,ser}}{2RT}\left(1-e^{-10}\right)$
S_{CR1}	0 (Soft Switching)	$\frac{2 I_L V_{on,sw} T_{C+}}{\pi T} + \frac{I_L{}^2 R_{on,sw} T_{C+}}{2T}$
SCR_6	0 (Soft Switching)	$\frac{I_L V_{on,sw} T_{C+}}{\pi T} + \frac{I_L{}^2 R_{on,sw} T_{C+}}{4T}$
$SCR_2 - SCR_5$	0 (Soft Switching)	$\frac{I_L V_{on,sw} \sqrt{L.C}}{T} + \frac{R_{on,sw} \sqrt{L_r.C}}{2T}$
$D_1 - D_4$	It is considered Zero	$\frac{2 I_L V_{on,D} T_{C+}}{1\,4\,2\,\frac{\pi}{a}T\,4\,3} + \frac{I_L{}^2 R_{on,D} T_{C+}}{1\,4\,2\,\frac{2}{b}T\,4\,3}$ $\frac{1}{n} a + \left(\frac{1}{n}\right)^2 b$

According to the values of inductor and capacitors, time constant for fully charging of the capacitors is 5 µs. After T_{C^+} = 5us, the maximum voltage of the capacitors will reach 50 volts. For generating positive pulse, polarities of the odd capacitors are changed. Thus, voltage of the odd capacitors will be -50 volts. When S_2 is turned on, 200 volts (voltage summation of the four capacitors) will be generated. By the same way, polarities of the even capacitors are changed to have the same voltage with negative polarity. According to the value of load resistor and C_s, the generated pulse reaches zero after time constant To. The simulation results, including current of inductor L_1, voltages of the capacitors, current of the resonant inductor are shown in Fig. 9 and output voltage, and voltage

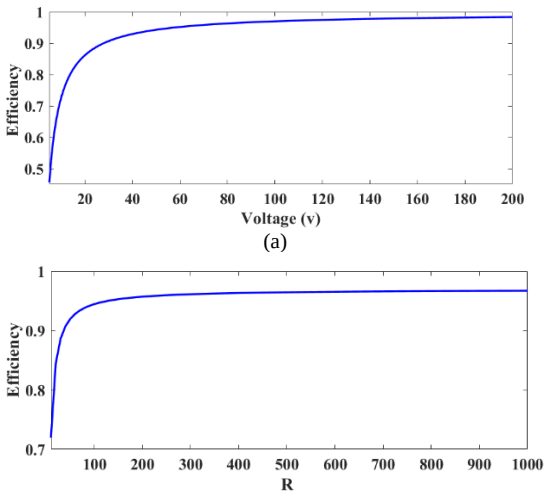

(a)

(b)

Fig. 8. The efficiency of the proposed structure a) the efficiency versus input voltage (v) b) the efficiency versus output resistor (Ω).

Table 4. Value of Proposed Structure Parameters in Simulation mode.

$V_{in}(v)$	$L_1(mH)$	$L_{2,3}(mH)$	$C_i(nF)$	$R_{load}(\Omega)$	ΔT(µs)
10	2	100	4.7	680	30

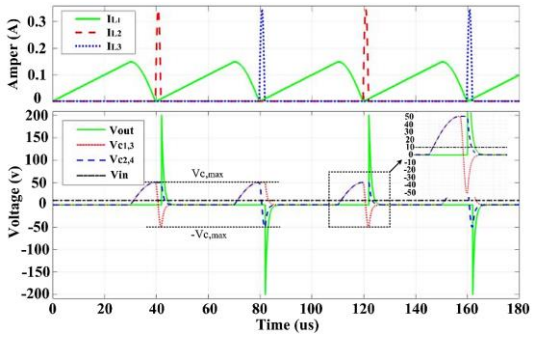

Fig. 9. The Inductors current, input voltage, output voltage and voltage of capacitors.

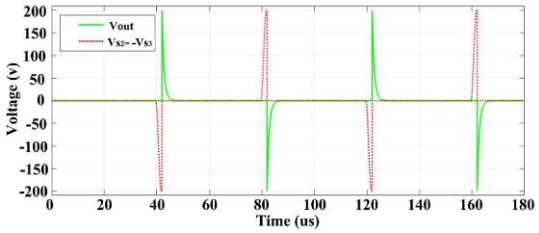

(a)

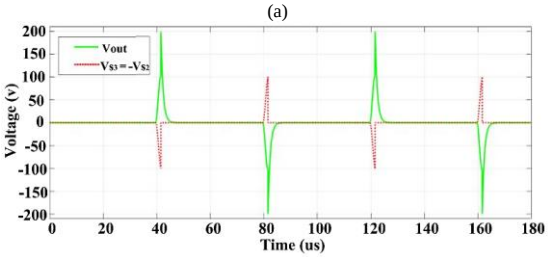

(b)

Fig. 10. The output voltage and the voltage generated on the switch S_2 and S_3 a) before adding SCR_7 b) after adding SCR_7.

across S_2 and S_3, in both the explained states are illustrated in Fig. 10.

6. CONCLUSION

In this paper, a new bipolar Marx generator was proposed, in which a buck-boost converter for improving the performance is employed. This converter can charge the capacitors up to several times of the conventional Marx generators. In the proposed structure, all the capacitors are charged at the same time. Then, with a small inductor through a resonant circuit, polarities of the even and odd capacitors are changed, respectively. After that, using two switches $\boldsymbol{S_2}$ and $\boldsymbol{S_3}$, voltage summation of the capacitors is applied to the output terminals. The applied voltage is reduced to half using an anti-parallel thyristor with $\mathbf{SCR_6}$. Modular capability of the proposed structure provides higher voltages without changing the voltage rating of the switches. The performance of the proposed structure was assessed using some simulations. All the corresponding simulation results comply with each other and prove the good performance of the proposed bipolar pulse generator.

7. REFERENCES

[1] T. Namihira, D. Wang, and H. Akiyama, "Pulsed power technology for pollution control," *Acta Phys. Pol. A*, vol. 115, no. 6, pp. 953–955, 2009.

[2] E. Gomez, D. A. Rani, C. R. Cheeseman, D. Deegan, M. Wise, and A. R. Boccaccini, "Thermal plasma technology for the

treatment of wastes: A critical review," *J. Hazard. Mater.*, vol. 161, no. 2, pp. 614–626, Jan. 2009.

[3] M. Naghizadeh, E. Farjah, T. Ghanbari, H. Pourgharibshahi, and M. T. Andani, "Efficient Grounding Method for DC Microgrid with Multiple Grounding Points," in *2018 Clemson University Power Systems Conference (PSC)*, Sep. 2018, pp. 1–6.

[4] M. Reberšek and D. Miklavčič, "Advantages and Disadvantages of Different Concepts of Electroporation Pulse Generation," *Automatika*, vol. 52, no. 1, pp. 12–19, Jan. 2011.

[5] J. C. Weaver and Yu. A. Chizmadzhev, "Theory of electroporation: A review," *Bioelectrochem. Bioenerg.*, vol. 41, no. 2, pp. 135–160, Dec. 1996.

[6] O. Yun, X.-A. Zeng, C. S. Brennan, and Z. Han, "Effect of Pulsed Electric Field on Membrane Lipids and Oxidative Injury of Salmonella typhimurium," *Int. J. Mol. Sci.*, vol. 17, no. 8, Art. no. 8, Aug. 2016.

[7] M. Naghizadeh, E. Farjah, and T. Ghanbari, "DC Microgrid Grounding Impact on Power Electronic Interfaces in Fault Condition," *IEEE Trans. Ind. Electron.*, vol. 67, no. 5, pp. 4120–4132, May 2020.

[8] M. Naghizadeh, E. Farjah, H. Samet, and T. Ghanbari, "Fault Tolerability of Power Electronic Interfaces, Impact of Grounding Architecture," in *2018 IEEE International Conference on Environment and Electrical Engineering and 2018 IEEE Industrial and Commercial Power Systems Europe (EEEIC / I&CPS Europe)*, Jun. 2018, pp. 1–6.

[9] O. Mirzapour, F. Mohammadi, and M. Sahraei-Ardakani, "Multidimensional Scenario Selection for Power Systems with Line and Generation Outages," in *2022 North American Power Symposium (NAPS)*, Oct. 2022, pp. 1–5.

[10] J. Lehr and P. Ron, *Foundations of Pulsed Power Technology*. John Wiley & Sons, 2017.

[11] L. M. Redondo, J. F. Silva, P. Tavares, and E. Margato, "High-voltage high-frequency Marx-bank type pulse generator using integrated power semiconductor half-bridges," in *2005 European Conference on Power Electronics and Applications*, Sep. 2005.

[12] L. M. Redondo, A. Kandratsyeu, and M. J. Barnes, "Marx Generator Prototype for Kicker Magnets Based on SiC MOSFETs," *IEEE Trans. Plasma Sci.*, vol. 46, no. 10, pp. 3334–3339, Oct. 2018.

[13] L. Lamy Rocha, H. Canacsinh, J. F. Silva, L. M. Redondo, and T. Luciano, "Modeling Marx generators for maximum pulse repetition rate estimation," in *2017 IEEE 21st International Conference on Pulsed Power (PPC)*, Jun. 2017, pp. 1–4.

[14] V. V. Tatur, "Modification of Marx generator with a doubling of output voltage," *Int. J. Circuit Theory Appl.*, vol. 43, no. 4, pp. 415–420, 2015.

[15] S. Zabihi, Z. Zabihi, and F. Zare, "A Solid-State Marx Generator With a Novel Configuration," *IEEE Trans. Plasma Sci.*, vol. 39, no. 8, pp. 1721–1728, Aug. 2011.

[16] H. Akiyama, T. Sakugawa, T. Namihira, K. Takaki, Y. Minamitani, and N. Shimomura, "Industrial Applications of Pulsed Power Technology," *IEEE Trans. Dielectr. Electr. Insul.*, vol. 14, no. 5, pp. 1051–1064, Oct. 2007.

[17] S. Zabihi, F. Zare, G. Ledwich, A. Ghosh, and H. Akiyama, "A new pulsed power supply topology based on positive buck-boost converters concept," *IEEE Trans. Dielectr. Electr. Insul.*, vol. 17, no. 6, pp. 1901–1911, Dec. 2010.

[18] M. Naghizadeh, H. S. Gohari, H. Hojabri, and E. Muljadi, "New Single–Phase Three-Wire Interlinking Converter and Hybrid AC/LVDC Microgrid," *IEEE Trans. Power Electron.*, vol. 38, no. 4, pp. 4451–4463, Apr. 2023.

[19] A. Elserougi, S. Ahmed, and A. Massoud, "A boost converter-based ringing circuit with high-voltage gain for unipolar pulse generation," *IEEE Trans. Dielectr. Electr. Insul.*, vol. 23, no. 4, pp. 2088–2094, Aug. 2016.

[20] M. Taherian, M. Allahbakhshi, E. Farjah, and H. Givi, "An Efficient Structure of Marx Generator Using Buck–Boost Converter," *IEEE Trans. Plasma Sci.*, vol. 46, no. 1, pp. 117–126, Jan. 2018.

[21] L. M. Redondo, H. Canacsinh, and J. F. Silva, "Generalized solid-state marx modulator topology," *IEEE Trans. Dielectr. Electr. Insul.*, vol. 16, no. 4, pp. 1037–1042, Aug. 2009.

[22] Mohadeseh Naghizadeh, Ebrahim Farjah, Teymoor Ghanbari, Eduard Muljadi, "Effect of Grounding Conditions on DC Microgrid Power Electronics Interfaces," 2023 IEEE Texas Power and Energy Conference (TPEC), College Station, TX, USA, 2023, pp. 1-6.

[23] H. Canacsinh, L. M. Redondo, and J. F. Silva, "Marx-Type Solid-State Bipolar Modulator Topologies: Performance Comparison," *IEEE Trans. Plasma Sci.*, vol. 40, no. 10, pp. 2603–2610, Oct. 2012.

[24] C. Yao, S. Dong, Y. Zhao, Y. Mi, and C. Li, "A Novel Configuration of Modular Bipolar Pulse Generator Topology Based on Marx Generator With Double Power Charging," *IEEE Trans. Plasma Sci.*, vol. 44, no. 10, pp. 1872–1878, Oct. 2016.

[25] S. Shakeri, M. Naghizadeh, and S. Esmaeili, "Identifying the Voltage Sags Vulnerability Area with Considering FACTS Devices," in *2020 28th Iranian Conference on Electrical Engineering (ICEE)*, Aug. 2020, pp. 1–5.

[26] A. A. Elserougi, A. M. Massoud, and S. Ahmed, "A Unipolar/Bipolar High-Voltage Pulse Generator Based on Positive and Negative Buck–Boost DC–DC Converters Operating in Discontinuous Conduction Mode," *IEEE Trans. Ind. Electron.*, vol. 64, no. 7, pp. 5368–5379, Jul. 2017.

[27] S. Ameli, M. J. Morshed, and A. Fekih, "Baseline Control Strategy for Maximum Power Tracking for a 5MW Offshore Wind Turbine," in *2019 IEEE Green Technologies Conference(GreenTech)*, Apr. 2019, pp. 1–6.

[28] A. Kazemtarghi, S. Dey, A. Mallik, and N. G. Johnson, "Asymmetric Half-Frequency Modulation in DAB to Optimize the Conduction and Switching Losses in EV Charging Applications," *IEEE Trans. Transp. Electrification*, pp. 1–1, 2023.